Journal of Biomolecular NMR, **22:** 37–46, 2002.
KLUWER/ESCOM

Solution structure of N-terminal SH3 domain of Vav and the recognition site for Grb2 C-terminal SH3 domain

Kenji Ogura[a], Koji Nagata[b], Masataka Horiuchi[a], Etsuko Ebisui[b], Tomoyo Hasuda[b,c], Satoru Yuzawa[a,c], Motohiko Nishida[a,c], Hideki Hatanaka[b] & Fuyuhiko Inagaki[a,c,*]
[a]*Graduate School of Pharmaceutical Sciences, Hokkaido University, Kita 12 Nishi 6, Kita-ku, Sapporo 060-0812, Japan;* [b]*Tokyo Metropolitan Institute of Medical Science, 3-18-22 Honkomagome, Bunkyo-ku, Tokyo 113-8613, Japan;* [c]*CREST, Japan Science and Technology Corporation, 4-1-8 Honmachi, Kawaguchi 332-0012, Japan*

Received 22 August 2001; Accepted 30 October 2001

Key words: Grb2, NMR, SH3 domain, tetra-proline region, Vav

Abstract

The three-dimensional structure of the N-terminal SH3 domain (residues 583–660) of murine Vav, which contains a tetra-proline sequence (Pro 607-Pro 610), was determined by NMR. The solution structure of the SH3 domain shows a typical SH3 fold, but it exists in two conformations due to *cis-trans* isomerization at the Gly614-Pro615 bond. The NMR structure of the P615G mutant, where Pro615 is replaced by glycine, reveals that the tetra-proline region is inserted into the RT-loop and binds to its own SH3 structure. The C-terminal SH3 domain of Grb2 specifically binds to the *trans* form of the N-terminal SH3 domain of Vav. The surface of Vav N-terminal SH3 which binds to Grb2 C-terminal SH3 was elucidated by chemical shift mapping experiments using NMR. The surface does not involve the tetra-proline region but involves the region comprising the n-src loop, the N-terminal and the C-terminal regions. This surface is located opposite to the tetra-proline containing region, consistent with that of our previous mutagenesis studies.

Introduction

Vav is a guanine nucleotide exchange factor (GEF) of the Rho/Rac family exclusively expressed in hematopoietic cells (Katzaf et al., 1989). Vav contains several functional domains characteristic to signal transducing proteins, including a calponin homology, a Dbl homology, a pleckstrin homology, a cystein rich domain and src homology regions with an SH3-SH2-SH3 in order. Numerous genetic analyses and biochemical studies have demonstrated that Vav plays pivotal roles in lymphocyte cell differentiation and proliferation, lymphokine production and cytoskeletal reorganization (Bustelo, 2000). These cellular responses are induced by extracellular stimuli to various types of receptors that trigger rapid tyrosine phosphorylation of Vav and enhance its guanine nucleotide exchange activity (Fischer et al., 1998).

*Author for correspondence. E-mail: finagaki@pharm.hokudai.ac.jp

Among the GEF family, Vav is unique in that it contains src homology regions (Pawson, 1995), and mutants that lack either of these regions lose transforming activity (Bustelo, 1996). The Vav SH2 domain has several targets, including ZAP-70 (Katzav et al., 1994) and EGFR (Bustelo et al., 1992, Margolis et al., 1992). The Vav C-terminal SH3 domain binds to hnRNP-K (Bustelo et al., 1995), Ku-70 (Romero et al., 1996) and zyxin (Hobert et al., 1996). However, except for growth factor receptor-bound protein 2 (Grb2), none of target proteins has been identified as a binding partner of Vav N-terminal SH3. A number of studies have demonstrated the formation of multimolecular complexes containing Vav and Grb2 in various cells (Bustelo, 2000) and this association is mediated through the Vav N-terminal SH3 domain (Vav nSH3) and the Grb2 C-terminal SH3 domain (Grb2 cSH3) (Ye and Baltimore, 1994; Ramos-Morales et al., 1995). For example, Vav-Grb2

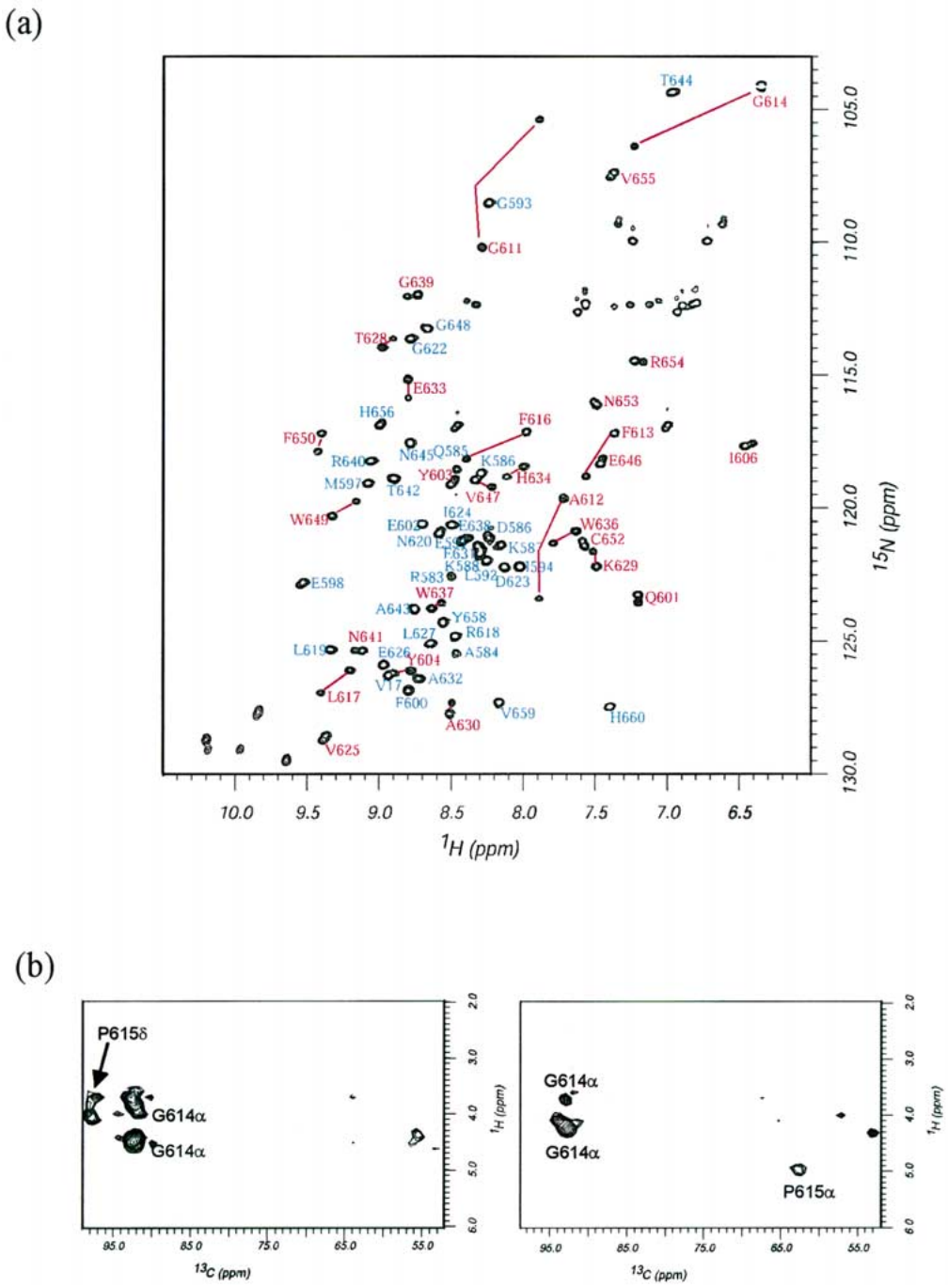

Figure 1. (a) ^{1}H-^{15}N HSQC spectrum of Vav nSH3 with peak assignments using one-letter amino acid codes. Several amino acid residues have double peaks, as shown by connecting lines. (b) Sliced subspectra from a 4D ^{13}C/^{13}C-edited NOESY spectrum of Vav nSH3 at (C^{α}, H^{α}) of Gly614. Sliced subspectra for the major peak (44.7 ppm, 4.49 ppm) and the minor peak (44.7 ppm, 4.21 ppm), are shown on the left and right, respectively. The assignments of the peaks are also shown.

complex is tethered to cholesterol-enriched membrane microdomains (GEM) from cytosol through binding of Grb2 to Linker of activation of T-cell (LAT) or CD28 (Simons and Ikonen, 1997; Bustelo, 2000). This process is important for tyrosine phosphorylation of Vav by T-cell or B-cell receptor associated tyrosine kinase, which is essential for cell proliferation.

Vav nSH3 contains a proline-rich region consisting of a tetra-proline sequence (Pro607-Pro610). Grb2 cSH3 was suggested to bind to Vav nSH3 through a classical PRR recognition mechanism as the binding was abrogated by double mutation at Pro608 and Pro610 (Ramos-Morales et al., 1995). However, a peptide containing the proline-rich sequence of Vav nSH3 did not bind to Grb2 cSH3, and, moreover, the binding requires both intact SH3 domains, suggesting that the Grb2-Vav interaction may be a novel mode of protein-protein interaction involving intact SH3 dimerization (Ye and Baltimore, 1994). These conflicting views prompted us to investigate the three-dimensional structure of Vav nSH3 in solution and in the crystalline state to elucidate the interaction with Grb2 cSH3. Here, we report the NMR results and compare them with those from X-ray crystallography (Nishida et al., 2001).

Materials and methods

The gene of the N-terminal SH3 domain of murine Vav (residues 583-660) (Vav nSH3) was cloned into the pHT-1 expression vector (Nagata et al., in preparation) using the *Nde*I and *Eco*RI restriction sites. Proteins were expressed in *E. coli* BLR(DE3)pLysS (Novagen, WI) cells. The P615G mutant, in which Pro615 was replaced by glycine, was prepared using a Quickchange Mutagenesis kit (Novagen, WI). Uniformly ^{15}N- and ^{13}C/^{15}N-labeled proteins were prepared by growing transformed *E. coli* cells in M9 medium containing CELTONE-CN (1 g l^{-1}) (Martek Biosciences, MD), $^{15}NH_4Cl$ (1 g l^{-1}) (Shoko, Tokyo) and [U-^{13}C]-glucose (2 g l^{-1}) (Shoko, Tokyo) in H_2O at 37 °C. Proteins were purified by affinity chromatography using His-Bind Resin (Novagen, WI), followed by the removal of the polyhistidine-tag by rTEV protease (Life Technologies, MD). The final purification of the polyhistidine-tag-removed proteins was achieved on a CHT-I (Bio-Rad, CA) ceramic hydroxyapatite chromatograph with a 10–100 mM linear gradient of potassium phosphate (pH 6.8). NMR samples contained 1.5 mM protein in a 10 mM potassium phosphate buffer (pH 6.8), and 10 mM DTT in $H_2O/^2H_2O$ (9:1) or ^2H_2O. The C-terminal SH3 domain of Grb2 (Grb2 cSH3) was prepared using a procedure described by Kohda et al. (1994).

All NMR spectra were recorded on Varian Unity-Plus 600 and Unity-Inova 500 spectrometers at 25 °C. The ^{1}H, ^{13}C and ^{15}N triple resonance spectra [HNCA, HN(CO)CA, CBCANH, CBCA(CO)NH, HBHA(CBCACO)NH, C(CO)NH] (Cavanagh et al., 1995) were obtained from samples in an H_2O buffer. The 4D HCCH-TOCSY (Olejniczak et al., 1992) spectrum was obtained from samples in a ^2H_2O buffer. The distance restraints were obtained from ^{15}N- or ^{13}C-edited 3D NOESY (Cavanagh et al., 1995) and ^{13}C/^{13}C-edited 4D NOESY (Cavanagh et al., 1995) spectra with 100 ms mixing time. {^{1}H}-^{15}N heteronuclear NOE (Kay et al., 1989) was measured using ^{15}N-labled protein in a H_2O buffer. All NMR spectra were processed with NMRPipe (Delaglio et al., 1995) and Felix 95.0 (Molecular Simulations, CA) programs.

Results and discussion

Trans and cis forms of Vav nSH3

The ^{1}H-^{15}N HSQC spectrum of Vav nSH3 shows well-resolved resonances (Figure 1a). However, the number of observed resonances is much larger than that expected for the Vav nSH3 construct (78 amino acid residues). The present observation indicates that Vav nSH3 exists in two conformations, a major and a minor forms, with an intensity ratio of approximately 2:1, and the conformation change between these two forms is slow on the NMR chemical shift time-scale. The main chain resonances of Vav nSH3 for the major and minor forms were subsequently assigned by an analysis of a suite of three-dimensional NMR experiments (Cavanagh et al., 1995). Interestingly, the residues that have two peaks with appreciable chemical shift differences (assigned to Gly611, Ala612, Phe613, Gly614, Phe616, and Leu617) encompass Pro615. Since the slow conformational change of proteins generally occurs through *cis-trans* isomerization at an X-Pro bond (Evans et al., 1987), Pro615 is the candidate most likely to be responsible for the two observed conformations. To confirm this, the 4D ^{13}C/^{13}C-edited NOESY spectra were analyzed. The sliced subspectra at the ^{1}H and ^{13}C chemical shifts of Gly614$^{\alpha}$ for the major and minor forms are shown

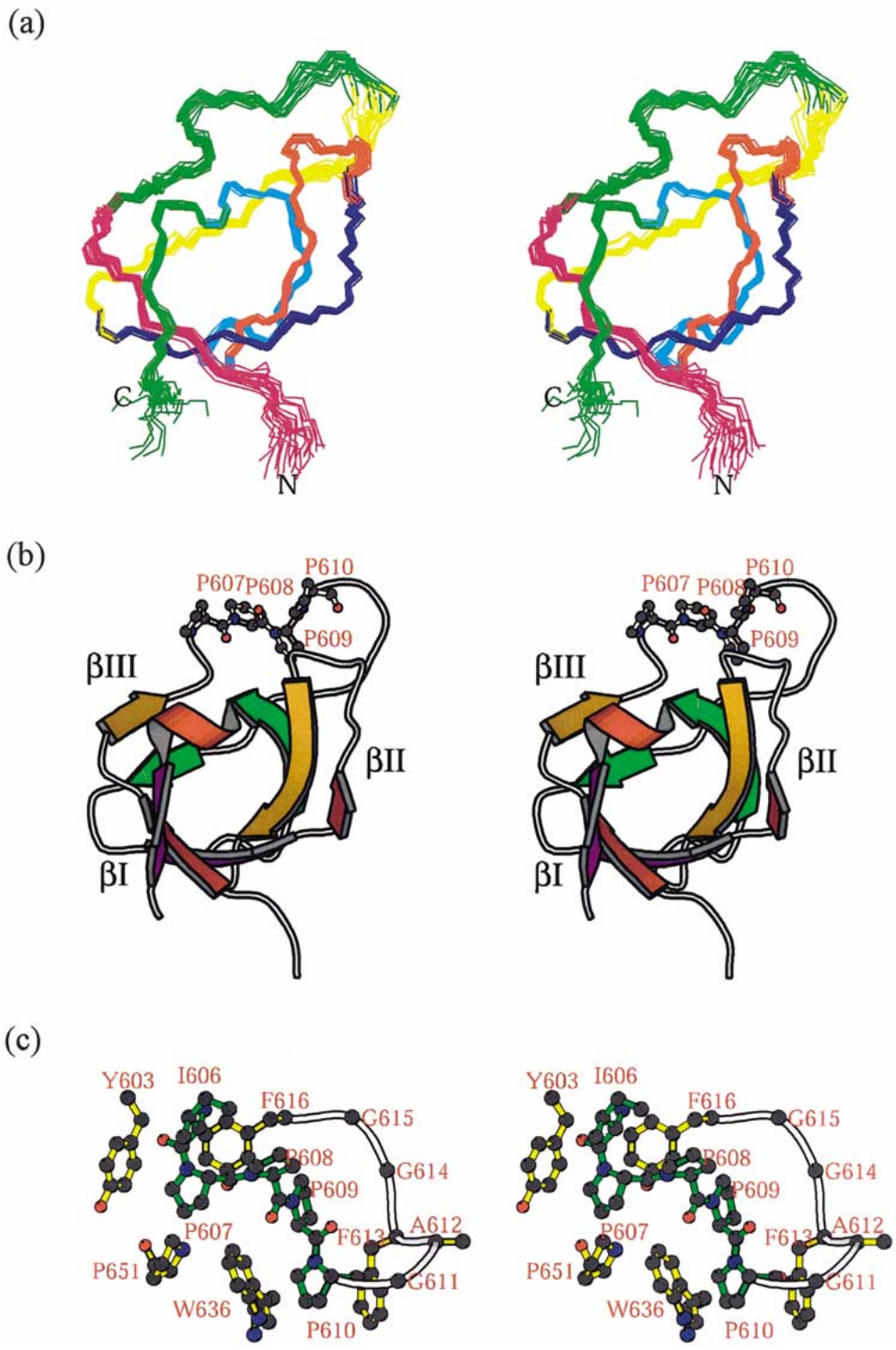

Figure 2. (a) Stereo-pair of overlays of the backbone (N, C^{α}, C') atoms of the 20 final solution structures of the P615G mutant. Color changes every 10 residues. The residues 593 and 658 are labeled with N and C to indicate the N- and C-terminus, respectively. (b) Ribbon diagram of the backbone (residues 593-659) conformation in the averaged structure of the P615G mutant. The tetra-proline region (Pro607-Pro610) is shown in a ball-and-stick model. (c) A close-up view of the tetra-proline region (green) and surrounding residues (yellow). Pro609 is stuck into the hydrophobic pocket formed by Trp636, Phe613 and Phe616. These figures are prepared using the Molscript program (Kraulis, 1991).

in Figure 1b. In the major form (left), we observed a NOE cross peak between Gly614$^{\alpha}$ and Pro615$^{\delta}$, while in the minor form (right), the NOE cross peak was between Gly614$^{\alpha}$ and Pro615$^{\alpha}$. Thus, the major and the minor forms are assigned to the *trans* and the *cis* forms at Gly614-Pro615, respectively. Subsequently, we prepared a mutant protein, P615G, in which Pro615 was replaced by glycine. In the ^{1}H-^{15}N HSQC spectra of the mutant protein, all the minor resonances disappeared, while the chemical shifts of almost all of the major resonances were unchanged. The binding affinity of the P615G mutant to Grb2 cSH3 was similar to that of the wild type (data not shown). Therefore, we concluded that the P615G mutant possesses essentially the same structure and biological activity as those of the *trans* form of the wild type.

The structure of the P615G mutant

The structures of the P615G mutant were calculated using an automated NOE assignment program, ARIA (Nilges and O'Donoghue, 1998) that has an interface with the CNS program (Brünger et al., 1998), based on the distance restraints obtained from 3D ^{15}N- or ^{13}C-edited NOESY spectra and the dihedral $\phi\psi$-angle restraints obtained from the program TALOS (Cornilescu et al., 1999). The experimental restraints, structural statistics and the structural evaluation using the program Procheck-NMR (Laskowski et al., 1996) are shown in Table 1. There were no NOE violations greater than 0.2 Å and no dihedral angle violations greater than 1.5° in the final structures. An overlay of the final ensemble of 20 simulated annealing structures is shown in Figure 2a.

The three-dimensional structure of the P615G mutant demonstrates the same general features as the canonical SH3 fold (Noble et al., 1993; Kohda et al., 1994; Eck et al. 1994). It consists of two triple-stranded antiparallel β-sheets (βI and βII) and a single turn of a 3_{10}-helix. An additional double-stranded antiparallel β-sheet (βIII) in the RT loop bends over the β-sandwich formed by the two other sheets (Figure 2b).

It should be noted that the tetra-proline sequence is inserted in the RT-loop, which is not fully exposed to the solvent but is fixed to the region close to the putative proline-rich peptide binding surface on the SH3 domain. A close-up view of the tetra-proline region together with surrounding residues is shown in Figure 2c. Pro609 is stuck into the pocket lined by Trp636, Phe613 and Phe616, while Pro608 is directed outward so that it does not interact with the SH3 domain. Pro607 interacts with Pro651 and Tyr603, and Pro610 with Phe613 and Trp636. Thus, the tetra-proline region is fixed by a number of hydrophobic interactions with the side chains of the SH3 domain. Ramachandran analysis using the program Procheck-NMR (Laskowski et al., 1996) gives the (ϕ, ψ) values of the proline-rich region as (−85°, 145°) for Pro607, (−64°, 153°) for Pro608, (−68°, 147°) for Pro609 and

Table 1. Experimental restraints and structural statistics for the 20 lowest energy structures

Number of experimental restraints	
Total unambiguous distance restraints	1282
Intra-residual	560
Sequential ($\|i-j\|=1$)	255
Medium range ($1<\|i-j\|<5$)	66
Long range ($\|i-j\|\geq 5$)	401
Hydrogen bonds	14
Ambiguous distance restraints	122
Dihedral restraints	
ϕ	44
ψ	36
Structural statistics	
RMSD from mean coordinate[a]	
Backbone (N, C^{α}, C') (Å)	0.27 ± 0.06
Heavy atoms (Å)	0.73 ± 0.41
RMSD from experimental restraints	
NOE distances (Å)	0.003 ± 0.001
Dihedral angles (deg.)	0.155 ± 0.04
RMSD from idealized geometry	
Bonds (Å)	0.001 ± 0.000
Angles (deg.)	0.249 ± 0.003
Impropers (deg.)	0.92 ± 0.12
Final energies (kcal/mol)	
E_{total}	51.07 ± 1.24
E_{bonds}	1.15 ± 1.10
E_{angles}	21.61 ± 0.47
$E_{impropor}$	0.92 ± 0.12
E_{vdw}	26.39 ± 1.23
E_{NOE}	0.87 ± 0.27
E_{cdih}	0.12 ± 0.06
Ramachandran analysis[b]	
Residues in most favored regions	85.0%
Residues in additionally allowed regions	15.0%
Residues in generously allowed regions	0
Residues in disallowed regions	0

[a]Calculated with the residues except for N-terminal (1–13), C-terminal (77 and 78), and a long RT-loop (23–33) regions.
[b]All the non-Gly/Pro residues for mean coordinate.

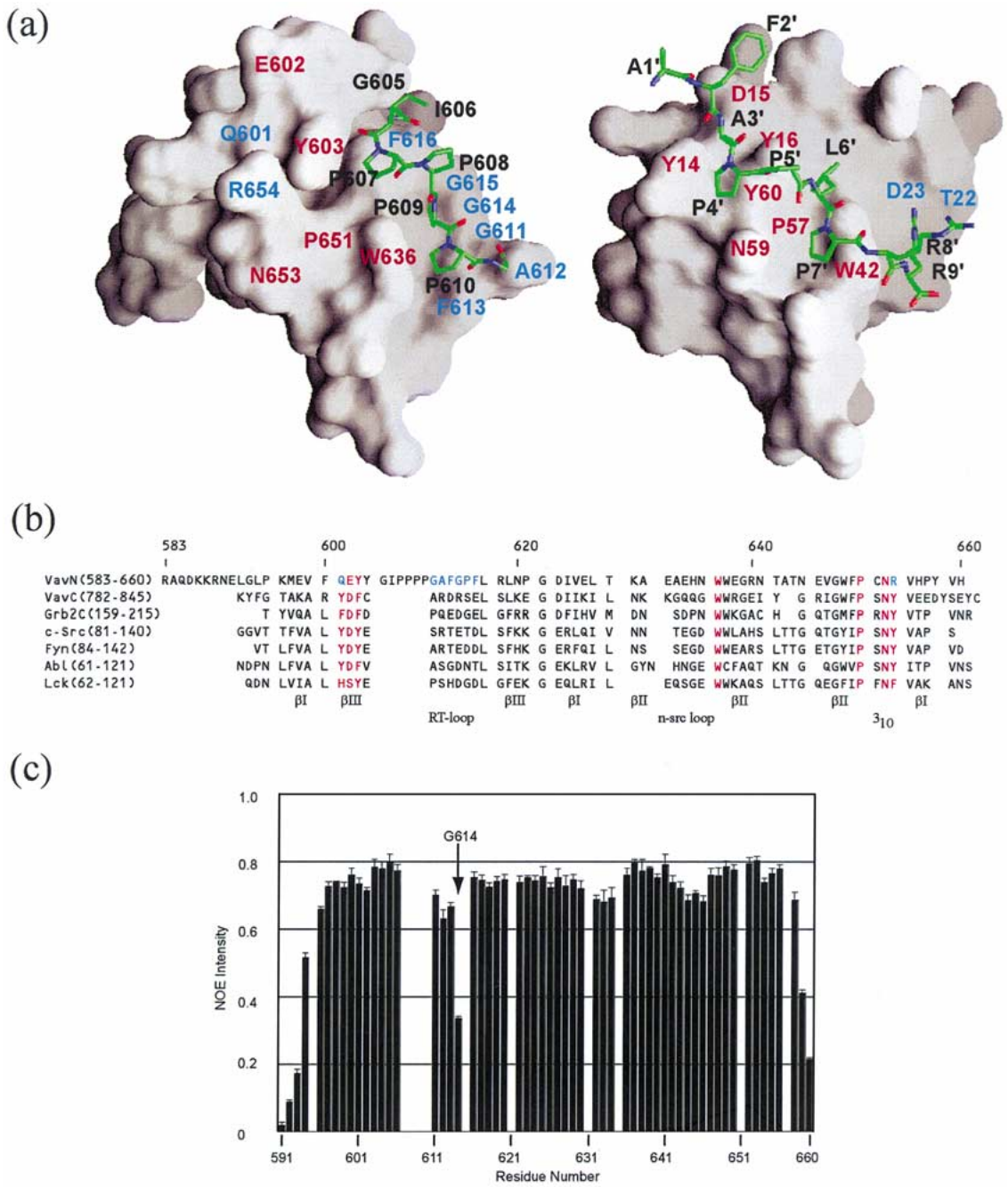

Figure 3. (a) Molecular surfaces of the P615G mutant (left) and the c-Src SH3 domain complexed with the peptide, AFAPPLPRRR (right). The surface of the P615G mutant was calculated excluding the residues of Ile606-Gly611. Residues 606–611 (left) and the binding peptides (right) are shown in the wire model (green). In both figures, the conserved and non-conserved residues forming the peptide-binding sites are shown in red and blue, respectively. These figures were prepared using the program Grasp (Nicholls et al., 1991). (b) Structure-based sequential alignment of SH3 domains. VavN, murine Vav N-terminal; VavC, murine Vav C-terminal; Grb2C, human Grb2 C-terminal; c-Src, chicken c-Src; Fyn, human Fyn; Abl, human Abl; Lck, human Lck. The assignments of the structural elements are shown at the bottom. Conserved residues in SH3 domains are shown in red. Residues that are highly conserved in SH3 domains but are replaced in Vav nSH3 are shown in blue. (c) $\{^1H\}$-^{15}N heteronuclear NOE values for individual residues of the *trans*-form of Vav nSH3. Gly614 is as flexible as the residues at the N or C-terminus, but the residues encompassing Gly614 are relatively rigid, suggesting the local flexibility of Gly614, which enables *cis-trans* isomerization at the Gly614-Pro615 bond. A similar tendency was observed in the *cis*-form.

(−74°, 146°) for Pro610, respectively. These four proline residues form the polyproline type-II helix, where Pro609 occupies the apex, while (Pro607, Pro608) and (Pro610, G611) occupy the basement of the polyproline type-II helix prism. It should be also noted that the Ile606-Pro607 bond takes a *cis* configuration.

Comparison of Vav nSH3 with c-src SH3

Figure 3a shows the protein surface of the P615G mutant (left) compared with that of c-Src SH3 bound to the ligand peptide, AFAPPLPRRR (PDB entry code: 1PRM) (right) (Feng et al., 1994). The surface of P615G mutant was calculated excluding the region from Ile606 to Gly611, upon which, the structure of Ile606-Gly611 is superposed with a wire model. The sequence alignment of the SH3 domains is also shown in Figure 3b. In c-Src SH3, the ligand-binding pockets are occupied by Ala3′, Pro4′, Leu6′, Pro7′ and Arg9′ of the peptide, respectively. The first binding pocket (site 1: P+3, P+2) of the SH3 domain is formed by Tyr14, Asn59 and Tyr60, and the second binding pocket (site 2: P0, P-1) consists of Tyr16, Trp42, Pro57, Asn59 and Tyr60. These six residues, which are highly conserved in the SH3 domains, play an important role in PXXP motif-recognition (Figure 3b). The third binding pocket (site 3: P-3) is formed by Thr22 and Asp23, which are highly variable residues located on the RT-loop, and generally binds the basic side chain of Arg9′. On the other hand, in P615G, the tetra-proline sequence is bound to the region close to, but different from site 2 and site 3 of the canonical SH3 domains. The region in P615G corresponding to site 1 is formed by Gln601 and Arg654, which are extremely conserved with aromatic residues in the SH3 domains (Figure 3b). While Trp636 and Pro651, which form site-2, are highly conserved residues in all SH3 domains. Pro607 binds to P0 through mainly hydrophobic interaction. In the canonical SH3 domains, site-3 consists of various acidic amino acid residues and binds basic residues of the peptide through electrostatic interaction. In contrast, in Vav nSH3, Pro610 is recognized by Ala612, Phe613 and Gly614. Since the putative proline-rich peptide binding region of Vav nSH3 is partially blocked by its own tetra-proline sequence and the canonical aromatic residues are replaced by Gln and Arg, Vav nSH3 appears to have no targets of proline rich sequences.

Structural flexibility of Vav nSH3

$\{^1H\}$-^{15}N heteronuclear NOE analysis of the *trans* form of Vav nSH3 revealed that Gly614, which is located in the RT-loop and close to the tetra-proline region (Pro607-Pro610), is flexible with a NOE value of 0.33 (Figure 3c). Although such flexibility is required for *cis-trans* isomerization of the Gly614-Pro615 bond, the residues on the RT-loop encompassing the tetra-proline region, including Gly605, Ile606, Gly611, Ala612, Phe613, Phe616 and Leu617, show large NOE values (around 0.7), indicating that the RT-loop is restrained except for Gly614. Similar observations were made concerning the $\{^1H\}$-^{15}N heteronuclear NOE values for the *cis* form. In both *trans* and *cis* forms, the RT-loop is relatively rigid except for the region at Gly614-Pro615. Based on the three dimensional structure of the P615G mutant, the tetra-proline region inserted in the RT-loop is bound on the surface of its SH3 domain, resulting in a partial masking of the ligand-binding pocket. In spite of local flexibility at the Gly614-Pro615 bond in both *cis* and *trans* forms, the tetra-proline region is fixed on the surface of the Vav nSH3 domain.

Interaction of Vav nSH3 with Grb2 cSH3

Interestingly, the tetra-proline region forms the polyproline type-II helix. The apex of the prism is stuck into the core of Vav nSH3, while the basement, which may be recognized by the target proteins, is exposed. Previous mutagenesis studies suggested that the tetra-proline region was recognized by Grb2 cSH3 in the classical manner (Ramos-Morales et al., 1995). However, there is contradicting experimental evidence. First, the binding is not abrogated by the peptide containing the tetra-proline region (Ye and Baltimore, 1994). Second, both intact SH3 domains are required for the binding (Ye and Baltimore, 1994). In order to elucidate the interaction between Vav nSH3 and Grb2 cSH3, we recorded a series of 2D ^1H-^{15}N HSQC spectra of uniformly ^{15}N-labeled Vav nSH3 (0.5 mM) upon addition of aliquots of Grb2 cSH3 stock solution, thus changing the molar ratio of Grb2 cSH3 to Vav nSH3 from 0 to 2. The cross peaks corresponding to the *cis* form disappeared upon complex formation with Grb2 cSH3. Thus, Grb2 cSH3 binds selectively to the *trans* form. The dissociation constant was estimated from the analysis of the binding curves by fluorescence intensity enhancement to be ca. 10 μM (data not shown). A number of residues displayed

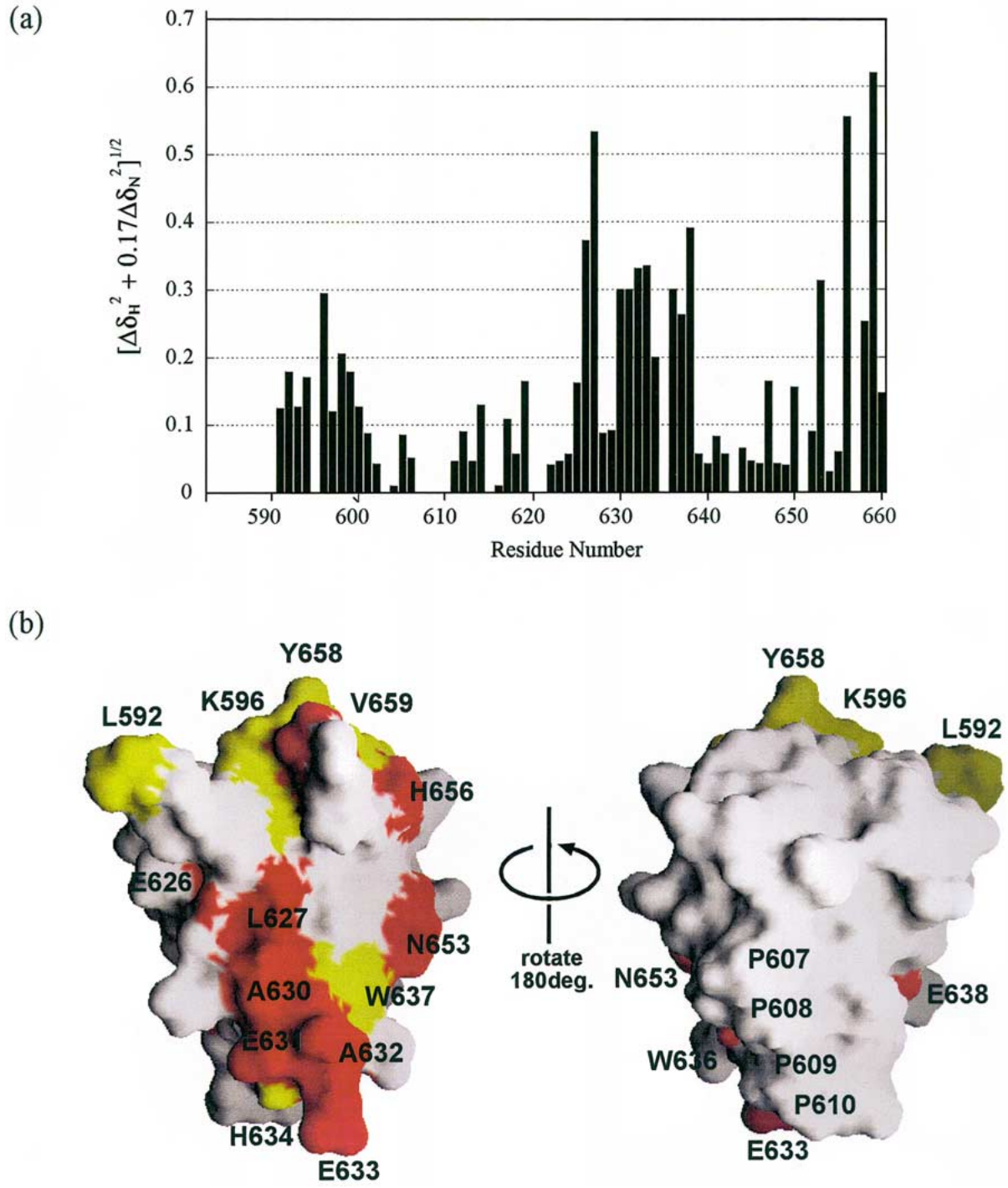

Figure 4. (a) The chemical shift changes of individual residues of ^{15}N labeled Vav nSH3 upon complex formation with Grb2 cSH3 as revealed by ^{1}H-^{15}N HSQC spectra. The weighted net changes in chemical shifts in ppm ($\Delta\delta = (\Delta\delta^2_{1HN} + 0.17\Delta\delta^2_{15N})^{1/2}$) are evaluated at the 1:2 molar ratio of Vav nSH3:Grb2 cSH3. (b) The Vav nSH3 residues affected by Grb2 cSH3 binding are mapped on the P615G mutant structure. The residues with large chemical shift changes are colored red (chemical shift changes is more than 0.3 ppm) and yellow (0.3–0.18 ppm), respectively. The tetra-proline region is indicated in (b). The left and right pictures are related by 180° rotation along y axis.

large chemical shift changes, while small but appreciable chemical shift changes were observed over the whole molecule, indicating the occurrence of a global conformation change upon complex formation (Figure 4a). When the residues with large weighted net change in chemical shifts of more than 0.18 ppm ($\Delta\delta = (\Delta\delta^2_{1HN} + 0.17\Delta\delta^2_{15N})^{1/2}$) (Vav nSH3:Grb2 cSH3=1:2) are mapped on the structure of Vav nSH3, they are found to be located in a specific region (Figure 4b), formed by the N-terminal region, C-terminal region, βI, βII and the n-src loop (left). While, on the opposite surface (Figure 4b, right), appreciable chemical shift changes were observed for Ala612, Gly614 and Leu617 which are located posterior to the tetra-proline region, while, the residues anterior to the tetra-proline region showed small chemical shift changes of less than 0.1 ppm. These results, taken together, led to the conclusion that the surface of Vav nSH3 opposite to the tetra-proline region (Figure 4b, left) was the major site for Grb2 cSH3 binding, although we could not precisely delineate the binding interaction. There may be a possibility that the tetra-proline region is the secondary binding site for Grb2 cSH3, nor do we neglect the possibility that the appreciable chemical shift changes on the RT-loop may be due to the conformation change induced by the Grb2 cSH3 binding. The interaction mode found in the present study is novel in that it is independent of the recognition of proline-rich sequence. The present results reconcile the conflicting experimental evidence. First, since the tetra-proline region is involved in a part of the structural core, double mutation in this region may disrupt the structure of Vav nSH3, thus decreasing the binding affinity (Ramos-Morales et al., 1995). Second, since the tetra-proline region is not a binding site for Grb2 cSH3, the peptide containing the tetra-proline region does not bind to Grb2 cSH3 (Ye and Baltimore, 1994) and does not disrupt the interaction of either molecule. Finally, since the binding surface is formed by the N-teminal and C-terminal regions as well as βI, βII and the 3_{10} helix, the binding requires the entire structure of Vav nSH3.

Recently, we have solved the crystal structure of the Vav nSH3-Grb2 cSH3 complex to elucidate the molecular interaction in detail (Nishida et al., 2001). In the crystal structure, there are two interaction surfaces on the Vav nSH3 domain corresponding to the tetra-proline region and the concave surface at the opposite side of the tetra-proline region. In the solution NMR study, H^N and N chemical shift values surrounding tetra-proline region of Vav nSH3 were not perturbed by Grb2-binding. Therefore we concluded that the interaction surface formed by tetra-proline region is an artifact by the crystal packing effect. This was consistent with our mutagenesis study (Nishida et al., 2001).

In conclusion, we demonstrated that Vav nSH3 has no target proline rich sequences, as the putative binding region is partially occupied by its tetra-proline region and the consensus aromatic residues are replcaed by more hydrophilic residues. In stead, Vav nSH3 develops a surface specifically prepared for Grb2 cSH3 binding. This binding mode is unique and requires the whole structure of Vav nSH3.

Coordinates

The coordinates of the minimized average structure of Vav nSH3 (P615G mutant) were deposited in the PDB with the accession code 1K1Z. The NMR chemical shifts were deposited at the BioMagResBank under accession code 5179.

Acknowledgements

This work has been supported by CREST of Japan Science and Technology (JST) and by a Grant-in-Aid for Scientific Research on Priority Areas from the Japan Ministry of Education, Science and Culture.

References

Brünger, A.T., Adams, P.D., Clore, G.M., DeLano, W.L., Gros, P., Grosse-Kunstleve, R.W., Jiang, J.S., Kuszewski, J., Nilges, M., Pannu, N.S., Read, R.J., Rice, L.M., Simonson, T. and Warren, G.L. (1998) *Acta Crystallogr. D Biol. Crystallogr.*, **54**, 905–921.

Bustelo, X.R. (1996) *Crit. Rev. Oncog.*, **7**, 65–88.

Bustelo, X.R. (2000) *Mol. Cell. Biol.*, **20**, 1461–1477.

Bustelo, X.R., Ledbetter, J.A. and Barbacid, M. (1992) *Nature*, **356**, 68–71.

Bustelo, X.R., Suen, K-L., Michael, W.M., Dreyfuss, G. and Barbacid, M. (1995) *Mol. Cell. Biol.*, **15**, 1324–1332.

Cavanagh, J., Fairbrother, W.J., Palmer, A.G. III and Skelton, N.J. (1995) *Protein NMR Spectroscopy*, Academic Press, San Diego, CA.

Cornilescu, G., Delaglio, F. and Bax, A. (1999) *J. Biomol. NMR*, **13**, 289–302.

Delaglio, F., Grzesiek, S., Vuister, G.W., Zhu, G., Pfeifer, J. and Bax, A. (1995) *J. Biomol. NMR*, **6**, 277–293.

Eck, M.J., Atwell, S.K., Shoelson, S.E. and Harrison, S.C. (1994) *Nature*, **368**, 764–769.

Evans, P.A., Dobson, C.M., Kautz, R.A., Hatfull, G. and Fox, R.O. (1987) *Nature*, **329**, 266–268.

Feng, S., Chen, J.K., Yu, H., Simon, J.A. and Schreiber, S.L. (1994) *Science*, **266**, 1241–1247.

Fischer, K-.D., Tedford, K. and Penninger, J.M. (1998) *Semin. Immunol.*, **10**, 317–327.

Hobert, O, Schilling, J.W., Beckerle, M.C., Ullrich, A. and Jallal, B. (1996) *Oncogene*, **12**, 1577–1581.

Katzaf, S., Martin-Zanca, D. and Barbacid, M. (1989) *EMBO J.*, **8**, 2283–2290.

Katzav, S., Sutherland, M., Packham, G., Yi, T. and Weiss, A. (1994) *J. Biol. Chem.*, **269**, 32579–32585.

Kay, L.E., Torchia, D.A. and Bax, A. (1989) *Biochemistry*, **28**, 8972–8979.

Kohda, D., Terasawa, H., Ichikawa, S., Ogura, K., Hatanaka, H., Mandiyan, V., Ullrich, A., Schlessinger, J. and Inagaki, F. (1994) *Structure*, **2**, 1029–1040.

Kraulis, P.J. (1991) *J. Appl. Crystallogr.*, **24**, 946–950.

Laskowski, R.A., Rullmann, J.A.C., MacArther, M.W., Kaptein, R. and Thornton, J.M. (1996) *J. Biomol. NMR*, **8**, 477–486.

Margolis, B., Hu, P., Katzav, S., Li, W., Oliver, J.M., Ullrich, A., Weiss, A. and Schlessinger, J. (1992) *Nature*, **356**, 71–74.

Nicholls, A., Sharp, K.A. and Honig, B.H. (1991) *Proteins*, **11**, 281–286.

Nilges, M. and O'Donoghue, S. (1998) *Prog. NMR Spectr.*, **32**, 107–139.

Nishida, M., Nagata, K., Hachimori, Y., Horiuchi, M., Ogura, K., Mandiyan, V., Schlessinger, J. and Inagaki, F. (2001) *EMBO J.*, **20**, 2995–3007.

Noble, M.E.M., Musacchio, A., Saraste, M., Courtneidge, S.A. and Wierenga, R.K. (1993) *EMBO J.*, **12**, 2617–2624.

Olejniczak, E.T., Xu, R.X. and Fesik, S.W., (1992) *J Biomol. NMR*, **2**, 655–659.

Pawson, T. (1995) *Nature*, **373**, 573–580.

Ramos-Morales, F., Romero, F., Schweighoffer, F., Bismuth, G., Camonis, J., Tortolero, M. and Fischer, S. (1995) *Oncogene*, **11**, 1665–1669.

Romero, F., Dargemont, C., Pozo, F., Reevers, W.H., Camonis, J., Gisselbrecht, S. and Fisher, S. (1996) *Mol. Cell. Biol.*, **16**, 37–44.

Simons, K. and Ikonen, E. (1997), *Nature*, 387, 569–572.

Ye, Z.S. and Baltimore, D. (1994) *Proc. Natl. Acad. Sci. USA*, **91**, 12629–12633.